

The controversial “Cambrian” fossils of the Vindhyan are real but more than a billion years older

Stefan Bengtson^{a,b,1}, Veneta Belivanova^a, Birger Rasmussen^c, and Martin Whitehouse^{b,d}

^aDepartment of Palaeozoology and ^dLaboratory for Isotope Geology, Swedish Museum of Natural History, SE-104 05 Stockholm, Sweden; ^bNordic Center for Earth Evolution, SE-104 05 Stockholm, Sweden; and ^cDepartment of Applied Geology, Curtin University of Technology, Perth, WA 6845, Australia

Edited by James P. Kennett, University of California, Santa Barbara, CA, and approved March 24, 2009 (received for review December 11, 2008)

The age of the Vindhyan sedimentary basin in central India is controversial, because geochronology indicating early Proterozoic ages clashes with reports of Cambrian fossils. We present here an integrated paleontologic–geochronologic investigation to resolve this conundrum. New sampling of Lower Vindhyan phosphoritic stromatolitic dolomites from the northern flank of the Vindhyan confirms the presence of fossils most closely resembling those found elsewhere in Cambrian deposits: annulated tubes, embryo-like globules with polygonal surface pattern, and filamentous and coccoidal microbial fabrics similar to *Girvanella* and *Renalcis*. None of the fossils, however, can be ascribed to uniquely Cambrian or Ediacaran taxa. Indeed, the embryo-like globules are not interpreted as fossils at all but as former gas bubbles trapped in mucus-rich cyanobacterial mats. Direct dating of the same fossiliferous phosphorite yielded a Pb–Pb isochron of $1,650 \pm 89$ (2 σ) million years ago, confirming the Paleoproterozoic age of the fossils. New U–Pb geochronology of zircons from tuffaceous mudrocks in the Lower Vindhyan Porcellanite Formation on the southern flank of the Vindhyan give comparable ages. The Vindhyan phosphorites provide a window of 3-dimensionally preserved Paleoproterozoic fossils resembling filamentous and coccoidal cyanobacteria and filamentous eukaryotic algae, as well as problematic forms. Like Neoproterozoic phosphorites a billion years later, the Vindhyan deposits offer important new insights into the nature and diversity of life, and in particular, the early evolution of multicellular eukaryotes.

geochronology | India | Mesoproterozoic | paleontology | Paleoproterozoic

The Vindhyan basin in Central India contains a thick unmetamorphosed sequence of sandstones, shales, and carbonate rocks together with volcanoclastic rocks (Fig. 1). Estimates of the age span of this Vindhyan Supergroup have varied considerably, but geochronologic evidence supports a Paleo- to Mesoproterozoic age [>1.7 to 1.6 billion years ago (Ga)] of the Lower Vindhyan (ref. 1 and references therein). Although a Neoproterozoic age has often been inferred for the Upper Vindhyan (1), firm geochronologic evidence for this has been missing, and recent paleomagnetic–geochronologic work even suggests a late Mesoproterozoic age (1.0 – 1.07 Ga) of the uppermost Vindhyan units (2).

These age assignments have been persistently challenged by reports of Ediacaran and Cambrian fossils from the Vindhyan rocks (3–8). In response to a claim for Mesoproterozoic animal trace fossils from the Lower Vindhyan Chorhat Sandstone at Chorhat (9), Rafat J. Azmi argued that the presence of Cambrian skeletal fossils in beds conformably overlying the Chorhat removed any need to postulate a Mesoproterozoic age (10). In the debate that followed (11–19), errors in Azmi’s reports were taken to suggest that they were fundamentally flawed and that the skeletal fossils did not exist (20).

Although most of Azmi’s fossils were convincingly reinterpreted as diagenetic artifacts (12), a few others remained as potential anomalies. Furthermore, recent publications by Azmi and coworkers (4, 5, 8) reported a number of apparently well-preserved Lower Vindhyan fossils closely resembling forms

previously known to be characteristic of the Cambrian: annulated tubes, embryo-like globules, and calcified cyanobacteria. If these and earlier reports are correct, they have profound implications: either the radiometric dating consistently reflects inherited dates not related to sedimentation, as suggested by Azmi and coworkers (4, 8), or Cambrian-like fossils occur in rocks that are a billion years older than the Cambrian. It is thus necessary to resolve the controversy.

Results

We performed an independent test of the veracity of Azmi’s fossil reports through renewed field sampling of the crucial rock sequences, subjecting them to integrated paleontologic–geochronologic analyses. The most significant results are from the Jankikund river section near Chitrakoot, on the northern flanks of the Vindhyan Plateau, which exposes unmetamorphosed phosphoritic stromatolite-bearing carbonate rocks of the Tirohan Dolomite Member of the Chitrakoot Formation. We provide independent confirmation of Azmi’s reports of Cambrian-like fossils in these rocks and present evidence that the fossils are indigenous to the rocks rather than contaminants. We further demonstrate by means of isotope geochemistry that the fossiliferous rocks were deposited more than 1.6 billion years ago and thus that the fossils indeed are more than a billion years older than the Cambrian.

Lithology and Sedimentology. The Jankikund rocks are stromatolitic carbonates, mainly dolostones, with phosphorite occurring as bands within and capping the stromatolites, and as intraclasts in the intercolumnar matrix. Glauconite grains, sometimes coated by phosphate envelopes, are also present. The fossils are found either directly in the phosphoritic intraclasts or as isolated phosphatic objects within the carbonates. Some portions of the rock are silicified, the silica occurring as botryoidal chert cement. Mineralogic, geochemical (21), and sedimentologic (22) studies of the Tirohan Dolomite indicate that it was deposited in a marine shallow subtidal to supratidal environment. Deposition near the air–water interface is also borne out by the common presence of gas bubbles, as discussed herein.

Microbial Fabrics. The phosphatic intraclasts typically have an irregular, tortured shape, largely governed by their microfabrics. Thus they were probably not strongly lithified at breakup. There is a diversity of clearly microbial fabrics (5), of which the most common type consists of tubular filaments forming dense bundles (Figs. 2 and 3A). The filaments are 10 – 35 μm in diameter,

Author contributions: S.B. designed research; S.B., V.B., B.R., and M.W. performed research; S.B., B.R., and M.W. analyzed data; and S.B. wrote the paper.

The authors declare no conflict of interest.

This article is a PNAS Direct Submission.

Data deposition: The figured specimens have been deposited at the Swedish Museum of Natural History, Stockholm, under the number series S156413–S156424.

¹To whom correspondence should be addressed. E-mail: stefan.bengtson@nrm.se.

This article contains supporting information online at www.pnas.org/cgi/content/full/0812460106/DCSupplemental.

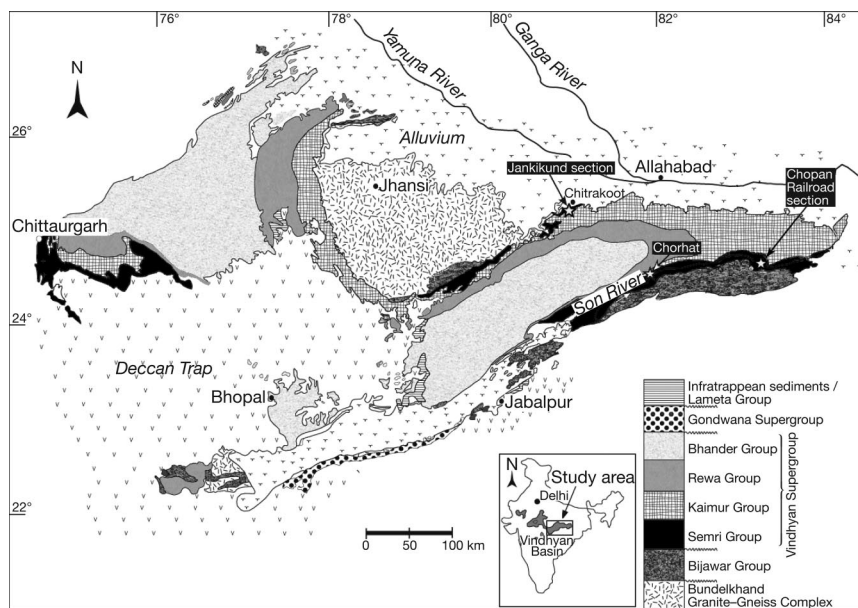


Fig. 1. Geologic map of the Vindhyan basin, central India. After Azmi et al. (4), based on several sources. Localities mentioned in the present study are labeled in white letters on black.

with 5–10- μm -thick walls made up of calcium phosphate and an internal cavity, approximately 1–15 μm wide, that may be empty or filled with carbonate.

The presence of diagenetic phosphatic cement in the clasts makes estimates of filament and wall thickness difficult and may also affect the apparent diversity. Spherulitic growth of the phosphate commonly produces cell-like structures that interfere with the original morphologies. However, the observed fabrics clearly represent microbial communities. The filamentous structures closely resemble fossil structures attributed to calcified filamentous cyanobacteria such as *Girvanella*, common in Phanerozoic, particularly Paleozoic, rocks (23). Known pre-Phanerozoic examples of calcifying cyanobacteria are scarce, being limited to a few Neoproterozoic 2.6–2.5 Ga (24, 25), Mesoproterozoic ≈ 1.2 Ga (26), and Neoproterozoic ≈ 0.8 Ga (27, 28) occurrences. The common criteria for distinguishing *in vivo* calcification from diagenetic mineralization (uniform wall thickness, nondegraded filaments) are inconclusive, however, particularly when the fossils occur in calcium phosphate, which has good potential of preservation of nonmineralized organic matter. The possibility therefore remains that the Jankikund filaments, despite their appearance, were noncalcified.

Embryo-Like Globules. Globular structures, with thin phosphatic walls, commonly with a granulated and occasionally with a polygonal surface pattern, are frequent in some Jankikund samples (Fig. 3). Such structures were interpreted as metazoan embryos by Azmi and colleagues (plates 2:11–13 of ref. 4), and individual specimens may indeed be superficially indistinguishable from the well-known embryos of Neoproterozoic–Cambrian transitional beds elsewhere (29, 30).

The combined features of the Jankikund globules make this interpretation unlikely, however. The diameter varies greatly, from approximately 30 μm to more than 1 mm, in sharp contrast to the constrained size range within individual taxa of metazoan embryo fossils (31). Jankikund globules occur both as isolated phosphatic objects in the carbonates (Fig. 3 *F* and *H*) and within phosphatic intraclasts that have a more-or-less distinct filamentous or coccoidal fabric (Fig. 3 *A*, *B*, *D*, and *E*). Globules of different sizes commonly occur together within clasts (Fig. 3*E*).

Larger globules may in such a situation be surrounded by smaller ones, and if the globules are tightly adpressed to one another, this arrangement produces a polygonal pattern on the surface of the larger globule (Fig. 3*B*). Where the bodies are closely adpressed to each other, they lose their spheroidal shape and become polyhedral (Fig. 3*D*). Some of the bodies have become flattened; the wall then shows a more-or-less complex pattern of concentric and other wrinkles (Fig. 3*C*).

The walls of the globules are approximately 10–15 μm thick, but the thickness is largely determined by secondary apatite overgrowth. The external surface is often smooth, but in addition to the occasional polygonal pattern there is commonly a coarsely granulated surface pattern of similar dimensions to the surrounding coccoidal fabric (Fig. 3*A*). The internal surface, as well as any internal material, is commonly overgrown with acicular and botryoidal apatite. The specimen in Fig. 3*H* has the remains of a smaller globule within the larger globules, the surfaces between them overgrown with apatite. Some specimens contain apatite-encrusted filaments (Fig. 3*F*) similar to the filamentous interior found in many phosphatized microfossils in Neoproterozoic–Cambrian phosphorites (32, 33).

Occasional aggregates show a smaller globular or tubular protrusion on each of the larger globules, always in the same direction within the same clast (Fig. 3*G*). This phenomenon is associated with radiating wrinkles in the fabric outside the protrusion.

We interpret the globular structures to be gas bubbles formed within cyanobacterial mats. This is borne out by their extensive size distribution and association with mat fabric; the occasional tubular protrusions would represent upward escape of gas through the wall of a bubble. Cyanobacteria release various gases, such as O_2 , CO_2 , and H_2 , as byproducts of respiration, photosynthesis, and nitrogen fixation (34), and the presence of large amounts of extracellular polymeric substances (EPS) in cyanobacterial mats promotes the trapping of bubbles. Mats are commonly loaded with gas bubbles, so that pieces of the mats may be torn and rafted away. Gas bubbles are only formed near the air–water interface, because higher hydrostatic pressures would keep the gases in solution (35).

Furniss et al. (figures 3 *B* and *D*, 4 *A* and *D*, 5*A*, and 6*C* of ref.

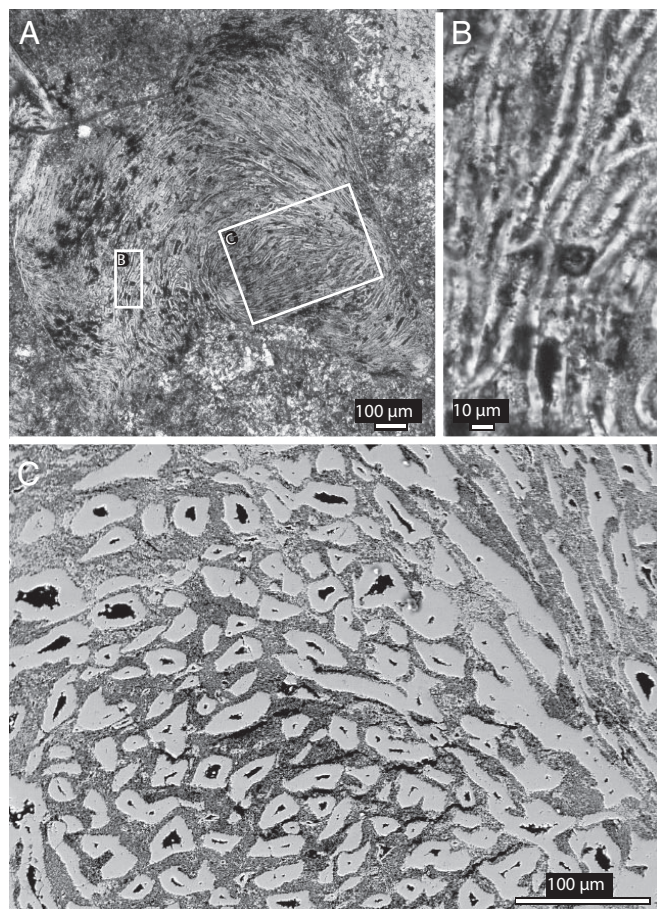


Fig. 2. Bundles of tubular filaments similar to calcifying cyanobacteria, in phosphorite clasts from the Jankikund section, sample Ind06110805. Thin section, S156413. (A and B) Transmitted light. (C) Back-scattered SEM image.

36) documented calcitic blobs with “nearly spherical to ovoid to angled, irregular shapes” in connection with “molar-tooth” structures in argillitic limestones and dolostones. They interpreted these to have been formed by gas in water-saturated muds. Experiments with bubbles formed by fermenting yeast in water-laden clay slurries produced closely similar structures (figure 4C of ref. 36); in both cases voids of submillimeter size were predominantly spheroidal in shape.

In the cases described by Furniss et al. (36), fossilization occurred through infill of the voids with calcite. In the case of the Jankikund phosphorites we envisage that the trapping of bubbles within an EPS matrix provided a means of fossilization through phosphatic replacement and/or overgrowth. Mucus is susceptible to preservation by mineralization by various mechanisms (37). Arp et al. (35) described the preservation of voids and bubbles through diagenetic mineralization of the EPS in modern cyanobacteria-dominated microbial mats. These mineralized bubbles show features that are closely similar to those observed in the Jankikund specimens, such as remnants of collapsed membrane within the bubble and acicular–botryoidal diagenetic minerals covering them as well as the inner surface of the bubble (compare figure 4A in ref. 35 with our Fig. 3H). The wrinkling of the surface in distorted Vindhyan specimens (Fig. 3C and G) also suggests that the shape of the bubble, as in the modern analogues, was upheld not only by surface forces at the gas–matrix interface but by a relatively resilient membrane.

Although the gas-bubble model seems able to explain most of the features of the Jankikund globules, and indeed in many cases

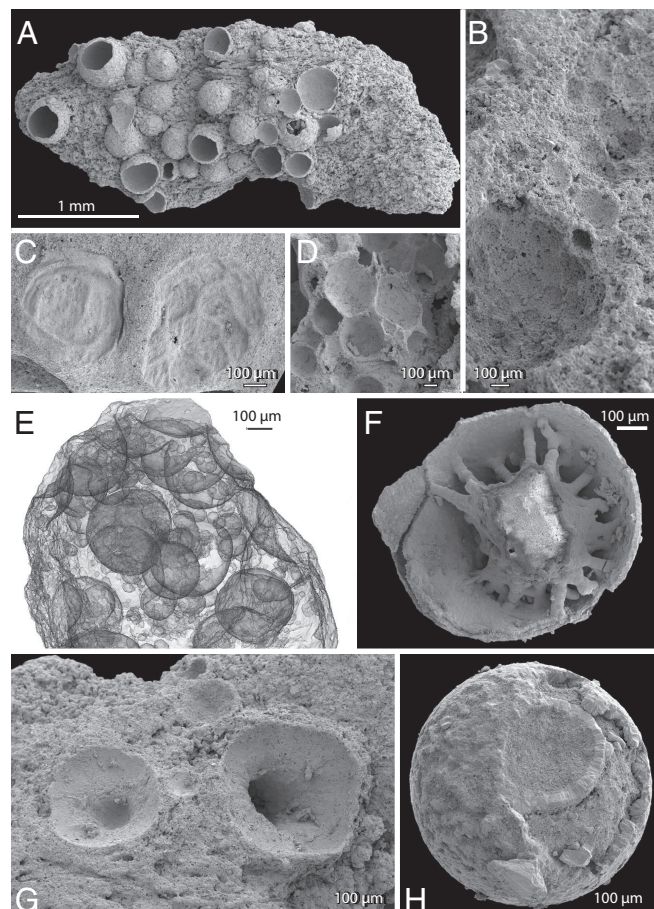


Fig. 3. Globular structures, interpreted as formed by gas bubbles within microbial mats, Jankikund section, sample Ind06110804. SEM (A–D, F–H) and SRXTM (E) images. (A) Globules of different size within filamentous fabric. S156414. (B) Negative casts of globules with polygonal surface structure, apparently formed by packing of smaller globules in matrix. S156415. (C) Two flattened globular objects with wrinkled surface membrane. S156416. (D) Packed globules forming foamy structure. S156417. (E) Clast containing foamy assemblage of globules of different sizes, viewed as transparent surface rendering of interfaces constructed by selective thresholding of gray-level values in voxel stack. S156418. (F) Globule with apatite-overgrown interior filamentous network. S156419. (G) Globules with probable gas escape structures. S156420. (H) Small globule within a larger one. Note palisade-like apatite overgrowth with occasional spherulitic structure. S156421.

it seems inescapable (see, e.g., the foamy fabric in Fig. 3D and E), other explanations for some of the globular structures cannot be excluded. The flattened wrinkled objects (Fig. 3C) may represent other organic structures, such as collapsed leiospherid achritarchs. The presence of phosphatized organic matter inside some bubbles (Fig. 3F) suggests more complex modes of formation than the mere growth of bubbles in an EPS matrix. Indeed, the strikingly embryo-like specimen from Rohtasgarh figured by Azmi et al. (plate 2:14 of ref. 4) as *Olivoides multisulcatus* is a strong indication that the bubble model cannot explain all globular structures in the Vindhyan sediments.

Segmented Tubes. Tubular objects approximately 100–180 µm in diameter occur sparsely in the Jankikund samples (Fig. 4). A distinct and consistent surface feature is a regular annulation consisting of shallow grooves perpendicular to the length axis, 60–140 µm apart. A few well-preserved specimens show the annulation to be expressions of transverse septa within the tubes (Fig. 4C). In these specimens, the volume of the space between

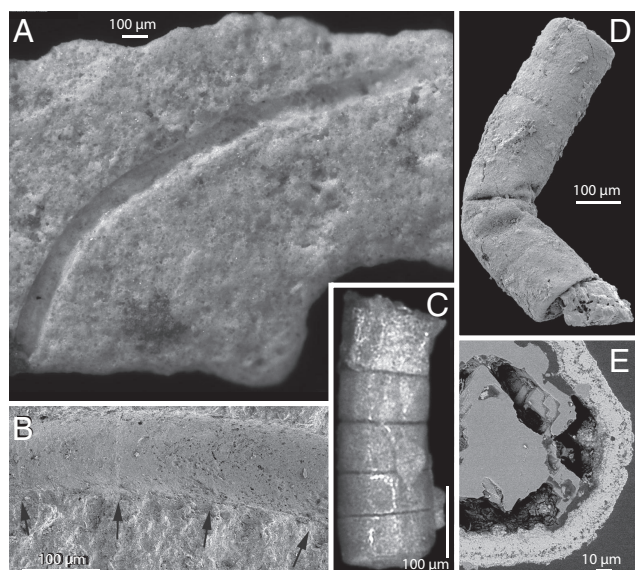


Fig. 4. Annulated and segmented tubes, Jankikund section, sample Ind06110804. Light (A and C) and SEM (B, D, and E) images. (A and B) Phosphorite clast with cast of 2-mm-long tube with weakly expressed annulations (arrows in B). S156422. (C) Tube with external annulations expressing transverse septa. S156423. (D and E) Tube with external annulations and evidence of prediagenetic plastic deformation. E is a back-scattered electron image of a polished transverse section through the tube. Note diagenetic apatite with spherulitic structure. S156424.

the septa varies from 0.8 to $1.9 \times 10^6 \mu\text{m}^3$. The tubes are frequently bent or distorted, and the accompanying wrinkling of the surface (Fig. 4D) shows that the original wall was thin and flexible. The fossilized wall consists of a layer of fibronormal apatite of varying thickness (Fig. 4E) and having an inward growth direction, consistent with a diagenetic encrustation on the inside of the original wall.

A flat phosphatic clast preserves the impression of a tube, 2 mm long and $100 \mu\text{m}$ in diameter (Fig. 4A and B), addressed parallel to the clast surface. There is no tapering, and weak annulations are present at distances approximately 80 – $140 \mu\text{m}$ apart (Fig. 4B, arrows). Morphologically it is thus indistinguishable from the shorter tubular segments present in the residues.

These tubes closely resemble annulated tubes reported by Azmi et al. as *Cambrotubulus decurvatus* and *Hyolithellus vladimirovae* (plates 1:1–4 of ref. 4). None of these named Cambrian taxa have transverse septa, however. Furthermore, their walls were mineralized and normally do not show the evidence of flexible bending or compression seen in the Vindhyan specimens. Thus we consider Azmi's identifications to be in error. Cambrian tubular fossils represent a wide diversity of morphology and composition and also include nonmineralized forms, but none of those presently known match the Vindhyan fossils.

In view of the extraordinary occurrence of phosphatized segmented tubes in rocks that may be more than a billion years older than the Cambrian, we considered carefully the possibility that these relatively rare fossils might be contaminations from other fossil samples or even the Recent biota. However, laboratory contaminations are unlikely given that we used new sieve sets that had never been in contact with Cambrian or other Phanerozoic samples and because our specimens conform closely with those reported by Azmi et al. (4). Contamination by Recent organisms living at the Jankikund site is also unlikely, because the tubes may be found in the phosphatic intraclasts that are part of the rock (Fig. 4A and B), and they are encrusted with diagenetic apatite similar to that found in the clasts (Fig. 4E).

Consequently, all of the available evidence indicates that the tubes are of the same age as the rock.

The septate nature of the Jankikund tubes precludes the interpretation that they represent extracellular sheaths of bacterial trichome bundles. The tubes resemble the concatenated cell walls of modern filamentous algae such as *Spirogyra*. The size of the cells is consistent with that of eukaryotic algae and several orders of magnitude larger than typical bacterial cells, the cytoplasmic volume of which is limited by diffusion requirements (38). However, certain sulfur-oxidizing bacteria exceed this size limit by filling up the cell volume with liquid vacuoles. Spherical *Thiomargarita* attain a cell volume of up to $2 \times 10^8 \mu\text{m}^3$, and filamentous *Beggiatoa* from hydrothermal-vent environments may form cylindrical cells up to $1 \times 10^6 \mu\text{m}^3$ in volume (38) (i.e., the same order of magnitude as in the Vindhyan tubes). Such dimensions are highly uncommon among bacteria, however.

The Lower Vindhyan Suket Shale in the Son River Valley, which is approximately stratigraphically equivalent to the Tirohan Dolomite, contains compressions of filamentous, occasionally branching fossils described as *Chambalia* (figure 14 a–e of ref. 39). They are of the same dimensions as the Jankikund tubes, but no internal structures or annulation are visible, so no direct comparison is possible. Compression fossils of what appears to be septate tubes have been reported from shales of the Paleoproterozoic Changcheng System as *Qingshania* (40). One large, parallel-sided specimen is 4.7 mm long and $216 \mu\text{m}$ wide, and 2 other specimens show a bulging terminal section (plates 3:4–5 of ref. 40). Judging from the published illustrations, the space between the septa attained a volume at least $6 \times 10^6 \mu\text{m}^3$. Again, this is considerably larger than most, although not all, bacteria.

Other Fossils. The Jankikund rocks contain a morphologic diversity of apparently biogenic objects. Those figured by Azmi et al. as *Mongolodus rostriformis*, *Halkieria* sp., *Protohertzina anabarica*, *Mongolodus platybasalis*, and *Rugatotheca* sp. (plates 1:9–13 and 2:4 of ref. 4) are readily included in the morphologic spectrum represented in our samples by fragments of microbial mats. There are also tubes and string-like objects similar to those that Azmi et al. (plates 1:6–8 and 2:5–10 of ref. 4) figured under the names *Anabarites trisulcatus*, *Protohertzina siciformis*, *Platysolenites antiquissimus*, *Cambrotubulus decurvatus*, and *Bathysiphon* sp. Some of these may be degraded specimens of the segmented tubes or diagenetically encrusted cyanobacterial filaments, but we cannot exclude that additional taxa are represented.

Thus we cannot confirm the presence of Cambrian taxa in the Vindhyan material. The characteristic elements are readily attributed to microbial fabrics, strings of concatenated cells, and gas bubbles. Nonetheless, the diversity of biogenic objects in our Jankikund samples, particularly the tubes and strings, indicate a greater fossil diversity than that represented by the microbial colonies and tubes reported herein. We also acknowledge that some of the forms reported by Azmi et al. (4) from other sections, in particular *Vindhyanitubulus semriensis*, *Olivoides multisulcatus*, *Orbisiana*, *Konglingiphyton* sp., and *Flabelliphyton strigata* from the Rohtasgarh Limestone in the Son River Valley (plates 2:1–3, 14, and 4:23–25 of ref. 4), strongly suggest an additional diversity of megascopic, morphologically distinct forms in the Lower Vindhyan. Additionally, the Vindhyan have a long history of megafossil discoveries (e.g., refs. 6 and 41–44) that sometimes have had difficulties getting into the mainstream literature because of uncertainties about the age, sometimes also because the reports themselves have not been convincingly documented. All these forms are highly significant for our understanding of biotic diversity in the Lower Vindhyan, but because our study concentrates on the Jankikund section, we do not deal with them in detail here.

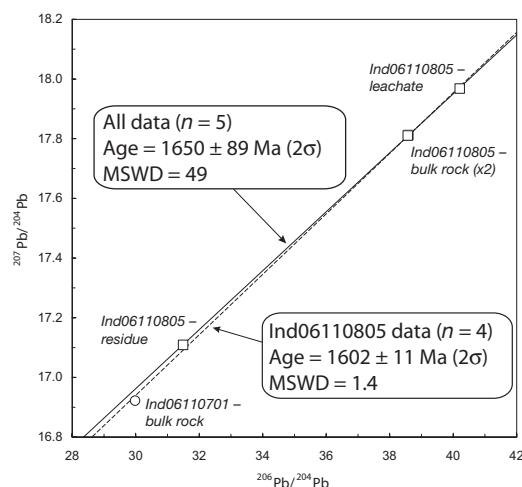


Fig. 5. Age regressions of Pb-isotope data from fossiliferous phosphorite from the Jankikund section, samples Ind 06110701 (circle) and Ind06110805 (squares). Analytic uncertainties are smaller than the symbol size. MSWD, mean square of weighted deviates.

Age. The geochronologic data on the Vindhyan Supergroup were recently reviewed by Ray (1) and by Azmi et al. (4, 8), who reached very different conclusions. Ray (1) cited recently published U–Pb dates from zircons (45, 46) and Pb/Pb isochrons from carbonates (47, 48), concluding that the Lower Vindhyan of the Son River Valley was deposited from before 1,721 million years ago (Ma) to approximately 1,600 Ma. Azmi et al. (4, 8) referred to the wide spread in published geochronologic dates from 1964 and onward, arguing that biostratigraphic constraints show the Lower Vindhyan to be Ediacaran to earliest Cambrian in age, the upper boundary given as <544 Ma. Azmi et al. considered the published older ages of approximately 1,600 Ma to reflect provenance of the sedimentary material, not deposition.

A further complication is added by the fact that the Chitrakoot sequence represents an outlier with uncertain correlation to the Lower Vindhyan sections elsewhere. Most of the published geochronologic dates are from the Son River Valley. Kumar et al. (49), however, reported Rb–Sr ages of $1,531 \pm 15$ Ma to $1,409 \pm 14$ Ma from glauconies in sandstones of the Chitrakoot region. The Tirohan Dolomite is not developed in that part of the Chitrakoot region; the sandstones probably represent lower stratigraphic levels.

Our assessment of the fossil assemblage at Jankikund has not revealed any biostratigraphic indicators of the Ediacaran or Cambrian. Nonetheless, given that *Girvanella*-like cyanobacteria such as those shown in Fig. 2 are exceedingly rare before the Cambrian (23), it is important to obtain independent evidence of the age of the fossiliferous rocks. We carried out Pb isotope analyses of the phosphorite intraclasts containing the fossils. The resulting Pb/Pb regression (Fig. 5) yields an age of $1,650 \pm 89$ (2σ) Ma for all analyses ($n = 5$), or $1,602 \pm 11$ (2σ) if only data from one sample are considered ($n = 4$). These age estimates are consistent with the U–Pb and Pb/Pb ages published from the Lower Vindhyan of the Son River Valley (reviewed in ref. 1) but older than the Rb–Sr ages from the glauconitic sandstones (49) of the Chitrakoot region. Because of the high susceptibility of ancient glauconite to thermal resetting, it is likely that these younger Rb–Sr dates represent postdepositional events and therefore provide minimum ages rather than depositional ages.

We further obtained U–Pb dates from zircons in tuffaceous mudrocks from the Porcellanite Formation (lower part of the Lower Vindhyan) in the Chopan Railway Section in the Son

River Valley [see Fig. 1 and [supporting information \(SI\)](#)]. The abundance of former glass shards along with quartz, K-feldspar, and minute euhedral zircon crystals indicates that the tuffaceous mudrocks were the products of explosive felsic volcanism. The dates obtained, $1,629 \pm 7$ (2σ) Ma and $1,626 \pm 7$ (2σ) Ma, are stratigraphically consistent with each other and with previous radiometric dates and indicate that the Porcellanite Formation was deposited in the late Paleoproterozoic.

In summary, there is strong and consistent evidence that the Lower Vindhyan sequence is Paleoproterozoic to early Mesoproterozoic in age. The direct dating by means of a Pb/Pb isochron of the fossiliferous lithology at Jankikund, in combination with the other geochronologic evidence, invalidates Azmi et al.'s proposal (4, 8) that the Lower Vindhyan biota is of Ediacaran–Cambrian age. The likely age of the biota is somewhere between 1,700 and 1,600 Ma, at the end of the Paleoproterozoic.

Discussion

Our results show that the fossil biota reported from the Lower Vindhyan of the Chitrakoot region by Azmi et al. (4) is indigenous to the rock rather than being due to sample contamination. We also demonstrate, however, that the published assignments of the fossils to Cambrian taxa of skeletal fossils are in error, and our new geochronologic work confirms a Paleoproterozoic age of the rocks.

The Lower Vindhyan thus presents a spectacular preservational window into a Paleoproterozoic biota. The main factors responsible for this preservation seem to be the low level of metamorphism, and—in the case of the Tirohan Dolomite—the presence of sedimentary phosphate, both unusual for rocks of this age. Phosphatization is often responsible for exquisite preservation of soft parts in the Neoproterozoic and Cambrian (29, 30, 50), whereas such preservation is comparatively uncommon in older and younger parts of the geologic column.

A long-standing problem in Precambrian paleobiology has been why calcifying cyanobacteria are so rare, compared with their massive occurrence in the Cambrian (51). This has been ascribed to high concentrations of dissolved inorganic carbon combined with low levels of Ca^{2+} in Proterozoic oceans (52), to high Proterozoic ambient CO_2 levels (23), or simply to preservational bias (53). The presence of *Girvanella*-like cyanobacteria in the Lower Vindhyan may help to elucidate levels of inorganic carbon in mat environments of the late Paleoproterozoic.

In terms of the evolution of major taxa, the most significant information to come out of the Vindhyan phosphorites is the detailed 3-dimensional morphologic evidence for late Paleoproterozoic multicellular eukaryotes (filamentous algae). Previously accepted multicellular eukaryotes were only known from the late Mesoproterozoic or early Neoproterozoic (54) (i.e., some 400–600 million years later), although some older discoveries had at least suggested the possibility that they had a longer prehistory (e.g., refs. 40, 55, and 56).

The potential of the Vindhyan phosphorites to yield fresh information on the Paleoproterozoic biotas is thus considerable, and the “shelly” biota discovered by Azmi et al. gives new insight into the nature of the Paleoproterozoic biosphere. The discredited reports of “Cambrian” fossils turned out to be an important discovery.

Materials and Methods

We visited and collected a number of Azmi's localities in November 2006, documented all sampling spots with photographs and global positioning system coordinates, packed the samples in the field, and shipped them directly to Stockholm and Perth for processing. For noncalcareous microfossil extraction, carbonate rocks were dissolved in 10% acetic acid. The acid-resistant residues were sieved and manually picked for microfossils. SEM was carried out on a Hitachi S4300 Field Emission scanning electron microscope. Synchrotron radiation x-ray tomographic microscopy (SRXTM) was performed on the X02DA TOMCAT

beamline at the Swiss Light Source, Paul Scherrer Institut, Villigen, Switzerland, with a beam energy of 17.5 keV, according to the procedures described by Donoghue et al. (57). Visualization was done with Avizo 5.1 (Mercury Computer Systems). For U–Pb dating of zircons, tuffaceous mudrocks were crushed, and heavy minerals were isolated using heavy liquids and magnetic separation. Data were collected with a sensitive high-resolution ion microprobe (SHRIMP). For Pb isotope analysis of the fossiliferous phosphorites, Pb was extracted from 2 whole-rock samples, as well as a leachate and residue pair, using conventional anion-exchange chromatography. The analysis was performed using an inductively coupled plasma multicollector mass spectrometer equipped with a desolvating nebulizer. Further details of sample treatment and analytical procedures are given in the SI.

1. Ray JS (2006) Age of the Vindhyan Supergroup: A review of recent findings. *J Earth System Sci* 115:149–160.
2. Malone SJ, et al. (2008) Paleomagnetism and detrital zircon geochronology of the Upper Vindhyan Sequence, Son Valley and Rajasthan, India: A ca. 1000 Ma closure age for the Purana Basins? *Precambrian Res* 164:137–159.
3. Azmi RJ (1998) Discovery of Lower Cambrian small shelly fossils and brachiopods from the Lower Vindhyan of Son Valley, Central India. *J Geol Soc India* 52:381–389.
4. Azmi RJ, et al. (2006) Age of the Vindhyan Supergroup of Central India: An exposition of biochronology vs radiochronology. *Micropaleontology: Application in Stratigraphy and Paleogeography*, ed Sinha D (Narosa Publishing House, New Delhi), pp 29–62.
5. Joshi D, Azmi RJ, Srivastava SS (2006) Earliest Cambrian calcareous skeletal algae from Tirohan Dolomite, Chitrakoot, Central India: A new age constraint for the Lower Vindhyan. *Gondwana Geol Magazine* 21:73–82.
6. De C (2006) Ediacara fossil assemblage in the upper Vindhyan of Central India and its significance. *J Asian Earth Sci* 27:660–683.
7. De C (2003) Possible organisms similar to Ediacaran forms from the Bhandar Group, Vindhyan Supergroup, Late Neoproterozoic of India. *J Asian Earth Sci* 21:387–395.
8. Azmi RJ, Joshi D, Tiwari BN, Joshi MN, Srivastava SS (2008) A synoptic view on the current discordant geo- and biochronological ages of the Vindhyan Supergroup, central India. *Himalayan Geol* 29:177–191.
9. Seilacher A, Bose PK, Pflüger F (1998) Triploblastic animals more than 1 billion years ago: Trace fossil evidence from India. *Science* 282:80–83.
10. Azmi RJ (1998) Fossil discoveries in India. *Science* 282:627.
11. Vishwakarma RK (1998) Cambrian life explosion in fray: Evidence from more than 1 b.y. old animal body fossils and skeletonization event. *Curr Sci* 75:1297–1300.
12. Conway Morris S, Jensen S, Butterfield NJ (1998) Fossil discoveries in India: Continued. *Science* 282:1265.
13. Swami Nath J, et al. (1999) Discussion: Discovery of Lower Cambrian small shelly fossils and brachiopods from the Lower Vindhyan of Son Valley, Central India. *J Geol Soc India* 53:120–131.
14. Tewari VC, et al. (1999) Discovery of Lower Cambrian small shelly fossils and brachiopods from the lower Vindhyan of Son Valley: Discussion and reply. *J Geol Soc India* 53:481–500.
15. Bhatt DK, et al. (1999) Fossil report from Semri Group, Lower Vindhyan. *J Geol Soc India* 53:717–723.
16. Srikantha SV (1999) Workshop on the Vindhyan stratigraphy and paleobiology, March 19–20, 1999, Lucknow. *J Geol Soc India* 53:724–726.
17. Brasier M, Azmi RJ (1999) Discovery of Lower Cambrian small shelly fossils and brachiopods from the lower Vindhyan of Son Valley: Discussion and reply. *J Geol Soc India* 53:727–730.
18. Ahluwalia AD, et al. (2000) Vindhyan fossil controversy. *J Geol Soc India* 55:675–680.
19. Bagla P (2000) Team rejects claim of early Indian fossils. *Science* 289:1273.
20. Kerr RA (1999) Earliest animals growing younger? *Science* 284:412.
21. Kumar S (1993) Mineralogy, geochemistry and genesis of middle Riphean phosphatic carbonates, Tirohan Limestone (Lower Vindhyan Supergroup), Chitrakut area, central India. *J Geol Soc India* 41:133–143.
22. Anbarasu K (2001) Facies variation and depositional environment of Mesoproterozoic Vindhyan sediments of Chitrakut Area, Central India. *J Geol Soc India* 58:341–350.
23. Riding R (2006) Cyanobacterial calcification, carbon dioxide concentrating mechanisms, and Proterozoic–Cambrian changes in atmospheric composition. *Geobiology* 4:299–316.
24. Klein C, Beukes NJ, Schopf JW (1987) Filamentous microfossils in the Early Proterozoic Transvaal Supergroup: Their morphology, significance, and paleoenvironmental setting. *Precambrian Res* 36:81–94.
25. Kazmierczak J, Altermann W (2002) Neoproterozoic biomining by benthic cyanobacteria. *Science* 298:2351.
26. Kah LC, Riding R (2007) Mesoproterozoic carbon dioxide levels inferred from calcified cyanobacteria. *Geology* 35:799–802.
27. Swett K, Knoll AH (1985) Stromatolitic bioherms and microphytolites from the late Proterozoic Draken Conglomerate Formation, Spitsbergen. *Precambrian Res* 28:327–347.
28. Halverson GP, Hoffman PF, Schrag DP, Maloof AC, Rice AHN (2005) Toward a Neoproterozoic composite carbon-isotope record. *Geol Soc Am Bull* 117:1181–1207.
29. Bengtson S, Yue Z (1997) Fossilized metazoan embryos from the earliest Cambrian. *Science* 277:1645–1648.
30. Xiao S, Zhang Y, Knoll A (1998) Three-dimensional preservation of algae and animal embryos in a Neoproterozoic phosphorite. *Nature* 391:553–558.
31. Steiner M, Zhu M, Li G, Qian Y, Erdtmann BD (2004) New Early Cambrian bilaterian embryos and larvae from China. *Geology* 32:833–836.
32. Yue Z, Bengtson S (1999) Embryonic and post-embryonic development of the Early Cambrian cnidarian *Olivoides*. *Lethaia* 32:181–195.
33. Pyle LJ, Narbonne GM, Nowlan GS, Xiao S, James NP (2006) Early Cambrian metazoan eggs, embryos, and phosphatic microfossils from northwestern Canada. *J Paleontol* 80:811–825.
34. Lindberg P, Lindblad P, Cournac L (2004) Gas exchange in the filamentous cyanobacterium *Nostoc punctiforme* strain ATCC 29133 and its hydrogenase-deficient mutant strain NHMS. *Appl Environ Microbiol* 70:2137–2145.
35. Arp G, Hofmann J, Reitner J (1998) Microbial fabric formation in spring mounds (“microbialites”) of alkaline salt lakes in the Badain Jaran sand sea, PR China. *Palaios* 13:581–592.
36. Furniss G, Rittel JF, Winston D (1998) Gas bubble and expansion crack origin of “molar-tooth” calcite structures in the Middle Proterozoic Belt Supergroup, Western Montana. *J Sediment Res* 68:104–114.
37. Dupraz C, Visscher PT, Baumgartner LK, Reid RP (2004) Microbe–mineral interactions: Early carbonate precipitation in a hypersaline lake (Eleuthera Island, Bahamas). *Sedimentology* 51:745–765.
38. Schulz HN, Jørgensen BB (2001) Big bacteria. *Annu Rev Microbiol* 55:105–137.
39. Kumar S (2001) Mesoproterozoic megafossil *Chuarina-Tawuia* association may represent parts of a multicellular plant, Vindhyan Supergroup, central India. *Precambrian Res* 106:187–211.
40. Yan YZ, Liu ZL (1993) Significance of eukaryotic organisms in the microfossil flora of Changcheng system. *Acta Micropalaeontol Sinica* 10:167–180.
41. Beer EJ (1919) Note on a spiral impression on Lower Vindhyan Limestone. *Rec Geol Surv India* 50:139.
42. Chapman F (1935) Primitive fossils, possible atrematous and neotrematous brachiopods, from the Vindhyan of India. *Rec Geol Surv India* 69:109–120.
43. Tandon KK, Kumar S (1977) Discovery of annelid and arthropod remains from Lower Vindhyan rocks (Precambrian) of Central India. *Geophytology* 7:126–129.
44. Kumar S (1995) Megafossils from the Mesoproterozoic Rohtas Formation (the Vindhyan Supergroup), Katni area central India. *Precambrian Res* 72:171–184.
45. Rasmussen B, et al. (2002) 1.6 Ga U–Pb zircon age for the Chhorhat Sandstone, lower Vindhyan, India: Possible implications for early evolution of animals. *Geology* 30:103–106.
46. Ray JS, Martin MW, Veizer J, Bowring SA (2002) U–Pb zircon dating and Sr isotope systematics of the Vindhyan Supergroup, India. *Geology* 30:131–134.
47. Ray JS, Veizer J, Davis WJ (2003) C, O, Sr and Pb isotope systematics of carbonate sequences of the Vindhyan Supergroup, India: Age, diagenesis, correlations and implications for global events. *Precambrian Res* 121:103–140.
48. Sarangi S, Gopalan K, Kumar S (2004) Pb–Pb age of earliest megascopic, eukaryotic alga bearing Rohtas Formation, Vindhyan Supergroup, India: Implications for Precambrian atmospheric oxygen evolution. *Precambrian Res* 132:107–121.
49. Kumar A, Gopalan K, Rajagopalan G (2001) Age of the Lower Vindhyan sediments, Central India. *Curr Sci* 81:806–809.
50. Müller KJ, Walossek D (1985) A remarkable arthropod fauna from the Upper Cambrian ‘Orsten’ of Sweden. *Trans R Soc Edinburgh Earth Sci* 76:161–172.
51. Riding R (1994) Evolution of algal and cyanobacterial calcification. *Early Life on Earth. Nobel Symposium 84*, ed Bengtson S (Columbia Univ Press, New York, NY), pp 426–438.
52. Arp G, Reimer A, Reitner J (2001) Photosynthesis-induced biofilm calcification and calcium concentrations in Phanerozoic oceans. *Science* 292:1701–1704.
53. Altermann W, Kazmierczak J, Oren A, Wright DT (2006) Cyanobacterial calcification and its rock-building potential during 3.5 billion years of Earth history. *Geobiology* 4:147–166.
54. Javaux EJ (2007) The early eukaryotic fossil record. *Origins and Evolution of Eukaryotic Endomembranes and Cytoskeleton*, ed Jékely G (Landes Bioscience, Austin, TX), pp 1–19.
55. Han TM, Runnegar B (1992) Megascopic eukaryotic algae from the 2.1 billion-year-old Negaunee Iron-Formation, Michigan. *Science* 257:232–235.
56. Hofmann HJ (1994) Proterozoic carbonaceous compression (“metaphytes” and “worms”). *Early Life on Earth*, ed Bengtson S (Columbia Univ Press, New York, NY), pp 342–357.
57. Donoghue PCJ, et al. (2006) Synchrotron X-ray tomographic microscopy of fossil embryos. *Nature* 442:680–683.